

Norrie disease protein is essential for cochlear hair cell maturation

Yushi Hayashi^{a,b}, Hao Chiang^{a,b}, ChunJie Tian^{a,b}, Artur A. Indzhyklian^{a,b,c}, and Albert S. B. Edge^{a,b,c,d,1}

^aDepartment of Otolaryngology, Harvard Medical School, Boston, MA 02115; ^bEaton Peabody Laboratory, Massachusetts Eye and Ear, Boston, MA 02114; ^cProgram in Speech and Hearing Bioscience and Technology, Harvard Medical School, Boston, MA 02115; and ^dHarvard Stem Cell Institute, Harvard University, Cambridge, MA 02139

Edited by Jeremy Nathans, Johns Hopkins University School of Medicine, Baltimore, MD, and approved July 13, 2021 (received for review April 5, 2021)

Mutations in the gene for Norrie disease protein (*Ndp*) cause syndromic deafness and blindness. We show here that cochlear function in an *Ndp* knockout mouse deteriorated with age: At P3-P4, hair cells (HCs) showed progressive loss of *Pou4f3* and *Gfi1*, key transcription factors for HC maturation, and *Myo7a*, a specialized myosin required for normal function of HC stereocilia. Loss of expression of these genes correlated to increasing HC loss and profound hearing loss by 2 mo. We show that overexpression of the *Ndp* gene in neonatal supporting cells or, remarkably, up-regulation of canonical Wnt signaling in HCs rescued HCs and cochlear function. We conclude that *Ndp* secreted from supporting cells orchestrates a transcriptional network for the maintenance and survival of HCs and that increasing the level of β -catenin, the intracellular effector of Wnt signaling, is sufficient to replace the functional requirement for *Ndp* in the cochlea.

Norrie disease | Wnt signaling | cochlear hair cells

Norrie disease is an X-linked, recessive, inherited disease that can be caused by over 100 different mutations in the *NDP* gene (1). Major manifestations of the disease are bilateral blindness with a prominent intraocular mass (pseudoglioma) and avascularity of the retina, intellectual disability, and progressive sensorineural hearing loss beginning in adolescence (2, 3). *Ndp* belongs to the cystine knot growth factor superfamily and shows weak homology with transforming growth factor- β (TGF- β) (4). *Ndp* signals through frizzled protein 4 (*Fzd4*), a member of the *Fzd* family of proteins that signal for stabilization and nuclear translocation of cytoplasmic β -catenin in response to Wnt ligand binding (5–7). β -catenin combines with Tcf/Lef transcription factors, which mediate binding to DNA and transcriptional activation of effector molecules (8, 9). Because of its binding to *Fzd4* and activity mediated by β -catenin (10), *Ndp* is considered an atypical Wnt.

Loss of *Ndp*/*Fzd4* signaling in endothelial cells causes defective vascular growth in development, leading to chronic but reversible silencing of retinal neurons (11). In the cochlea, *Ndp* knockout (KO) mice exhibited enlarged vessels in the lateral wall at 3.2 mo and degenerated vessels and loss of hair cells (HCs) at 15 mo (12). Similarly, *Fzd4* KO mice showed enlarged vessels in the lateral wall at 4.5 mo and degeneration of vessels in the organ of Corti at 11 mo (13).

To better understand the pathophysiology of the disease, we sought to learn whether the HC deterioration could be a direct result of the defect in *Ndp* signaling. Given that hearing loss in Norrie disease progresses gradually with a median age of onset of 12 y (14), we expected that the effects of *Ndp* KO would only become apparent postnatally. Wnt signaling contributes to the differentiation of HCs from postnatal cochlear progenitor cells (15, 16), and the activity of *Ndp* as an alternative Wnt ligand has the potential to affect HCs directly. Because HCs as well as vessels show pathology in the *Ndp* or *Fzd4* KO mouse cochlea, we considered the possibility that the signaling cascade downstream of *Ndp* was important for HC survival and function.

Results

***Ndp* KO Mice Exhibited Progressive Hearing Loss.** Vascular degeneration has been noted in the cochlea of the *Ndp* KO mouse at 3 mo of age (12, 13), and cochlear pathology has been attributed to vascular insufficiency, similar to the case of the retina in Norrie disease (1, 11, 13, 17). We examined the cochlear phenotype of the *Ndp* KO mouse at younger ages to assess the progression of cochlear degeneration. We first measured the auditory brainstem response (ABR), an indicator of intact neural connections from HCs to the brainstem via the auditory nerve, and the distortion product otoacoustic emission (DPOAE), an indicator of outer HC (OHC) function. Male WT (X^+Y), male KO (X^-Y), female wild-type (WT) (X^+X^+), female heterozygous (X^+X^-), and female KO (X^-X^-) mice were assessed at 1, 2, and 6 mo. Male KO mice, the disease-relevant genotype, showed a 10-dB threshold shift in the ABR at 1 mo (Fig. 1A); increased thresholds indicate decreased auditory response, and ABR thresholds were profoundly elevated at 2 mo at all but the highest frequency tested (45.25 kHz; Fig. 1B). The ABR thresholds were further elevated at 6 mo (*SI Appendix, Fig. S1A*; WT male littermates, which comprised the background strain, C57BL/6, also had elevations at high frequencies, a known age-related phenotype). The DPOAE thresholds were progressively elevated at 1 and 2 mo (Fig. 1C and D). Female KO mice showed similar phenotypes in the ABR and DPOAE, whereas female heterozygous mice exhibited slowly progressing ABR threshold elevations at high frequencies only (Fig. 1E–H and *SI Appendix, Fig. S1B*). *Ndp* KO mice thus demonstrated progressive hearing loss without distinction by sex; the elevated DPOAE thresholds indicated dysfunction of OHCs, but a

Significance

Norrie disease causes deafness, blindness, and intellectual disability. By analyzing gene expression downstream of Norrie disease protein (*Ndp*), we show that *Ndp* controls a network of transcriptional regulators required for maturation and maintenance of cochlear hair cells. We demonstrate that *Ndp* secretion, after forced expression of the gene in cochlear supporting cells of *Ndp*-deficient mice, prevents the hearing-loss phenotype exhibited by these mice. Moreover, forced activation of the canonical Wnt pathway mediator, β -catenin, in hair cells is sufficient to rescue hearing, demonstrating that *Ndp* secreted from supporting cells acts on adjacent hair cells and is required for the maturation and continued functioning of these cells.

Author contributions: Y.H., H.C., A.A.I., and A.S.B.E. designed research; Y.H., H.C., C.T., and A.A.I. performed research; Y.H., H.C., C.T., A.A.I., and A.S.B.E. analyzed data; and Y.H. and A.S.B.E. wrote the paper.

The authors declare no competing interest.

This article is a PNAS Direct Submission.

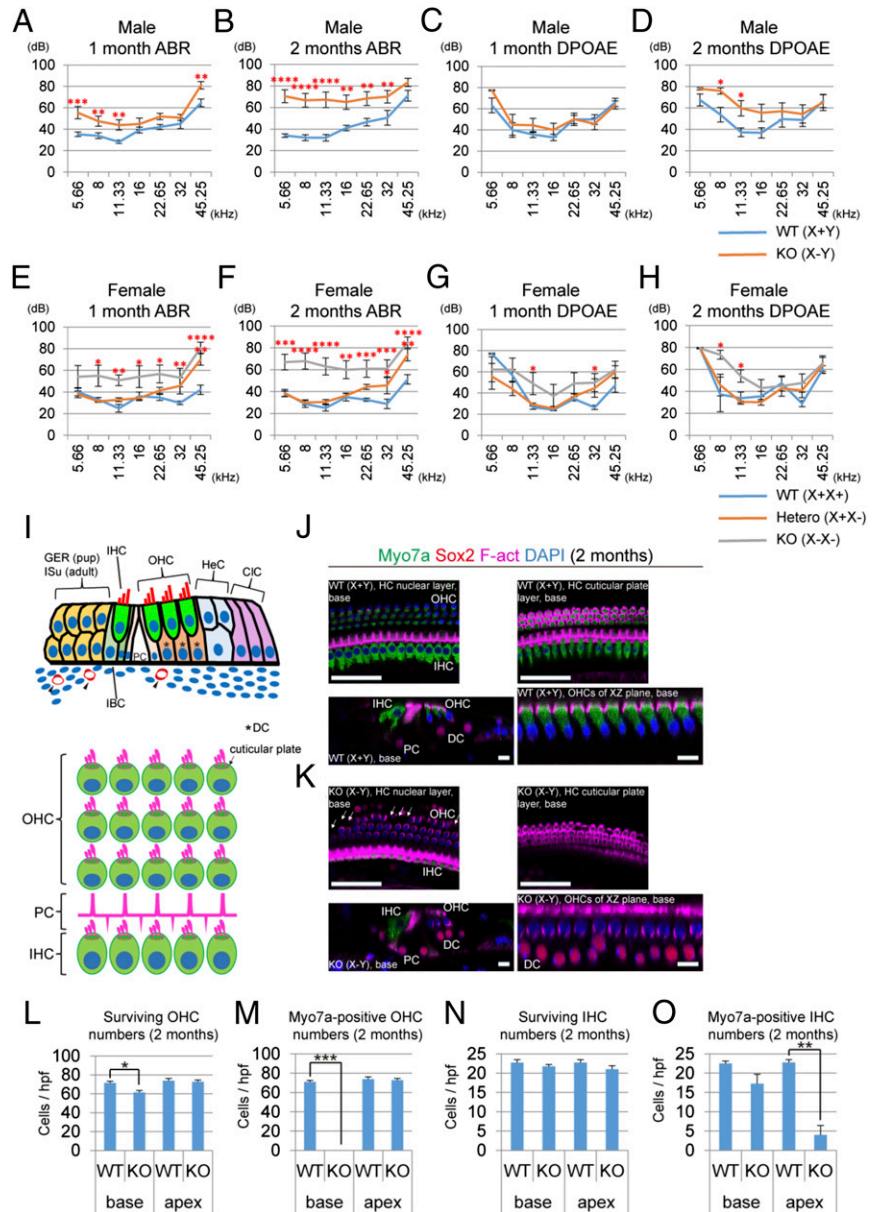
Published under the PNAS license.

¹To whom correspondence may be addressed. Email: albert_edge@meei.harvard.edu.

This article contains supporting information online at <https://www.pnas.org/lookup/suppl/doi:10.1073/pnas.2106369118/-DCSupplemental>.

Published September 20, 2021.

Fig. 1. *Ndp* KO mice exhibit progressive hearing loss and OHC death. (A) ABR thresholds were increased in male KO (X⁻Y) mice at 1 mo (WT: *n* = 14, KO: *n* = 10; *P* < 0.0001, ANOVA; post hoc tests at 5.66, 8.00, 11.33, and 45.25 kHz). (B) ABR threshold elevations in KO mice were more severe at 2 mo (WT: *n* = 10, KO: *n* = 9; *P* < 0.0001, ANOVA; post hoc tests at all frequencies except 45.25 kHz). (C and D) DPOAE thresholds in KO mice were unchanged at 1 mo (C, WT: *n* = 14, KO: *n* = 10; *P* < 0.0001, ANOVA) but were elevated at 2 mo (D, WT: *n* = 10, KO: *n* = 9; *P* < 0.0001, ANOVA; post hoc tests at 8.00 and 11.33 kHz). (E) ABR thresholds were increased across frequencies in female KO (X⁻X⁻) mice and at high frequencies in heterozygous (X⁻X⁺, Hetero) mice at 1 mo (WT: *n* = 5, Hetero: *n* = 7, KO: *n* = 6; *P* < 0.0001, ANOVA; post hoc tests at 8.00, 11.33, 16.00, 22.65, 32.00, and 45.25 kHz in KO mice and at 45.25 kHz in heterozygous mice). (F) ABR thresholds were further elevated across frequencies in female KO mice and at 32.00 and 45.25 kHz in heterozygous mice at 2 mo (WT: *n* = 4, Hetero: *n* = 7, KO: *n* = 5; *P* < 0.0001, ANOVA; post hoc tests at 5.66, 8.00, 11.33, 16.00, 22.65, 32.00, and 45.25 kHz in KO mice and at 32.00 and 45.25 kHz in heterozygous mice). (G and H) DPOAE thresholds in KO mice were elevated at 1 mo (G, WT: *n* = 5, Hetero: *n* = 7, KO: *n* = 6; *P* < 0.0001, ANOVA; post hoc tests at 11.33 and 32.00 kHz in KO mice) and were further elevated at 2 mo in KO mice (H, WT: *n* = 4, Hetero: *n* = 7, KO: *n* = 5; *P* < 0.0001, ANOVA; post hoc tests at 8.00 and 11.33 kHz in KO mice). (A–H) Error bars represent SEs. **P* < 0.05, ***P* < 0.01, ****P* < 0.001, *****P* < 0.0001 by Fisher's least significant difference method. (I) Diagrams of the organ of Corti including HCs, supporting cells, and blood vessels (arrowheads) (Upper: section view, YZ plane; Lower: surface view, XY plane; greater epithelial ridge: GER, inner sulcus: ISu, inner border cell: IBC, pillar cell: PC, Deiters' cell: DC, Hensen's cell: HeC, Claudius' cell: CIC, inner hair cell: IHC, and outer hair cell: OHC). (J) In the WT, HCs were positive for Myo7a at the base of the cochlea in both nuclear and cuticular plate layers. Computational sections showed Myo7a-positive HCs (PCs and DCs) are positive for Sox2, a supporting cell marker. (K) In the KO, many OHCs at the base of the cochlea were negative for Myo7a as viewed in the nuclear layer, with weak positive immunoreactivity in the cuticular plate layer, and some OHCs were missing (arrows). Computational sections showed Myo7a-negative OHCs in the base. (J and K) (Scale bars in whole mounts and computational sections indicate 50 and 10 μm, respectively.) (L and M) Significant loss of OHCs (L) and decreased numbers of Myo7a-positive OHCs (M) were observed at the base of the KO (*n* = 4) compared to the WT (*n* = 4) cochlea. No loss of OHCs was observed at the apex. Cell numbers are given as cells/high-power field (hpf). (N and O) No loss of IHCs was observed in the KO cochlea (N), but a tendency toward decreased numbers of Myo7a-positive IHCs in the base and a significant decrease in Myo7a-positive IHCs in the apex in the KO (*n* = 4) as compared to the WT (*n* = 4) cochlea were observed (O). (L–O) Error bars represent SEs. **P* < 0.05, ***P* < 0.001, ****P* < 0.0001.



further decrease in cochlear function from another source such as inner HCs (IHCs) or afferent neurons was evident from the greater magnitude of the threshold shifts in the ABR.

Myo7a-Negative HCs and HC Death in the *Ndp* KO Mouse Cochlea at 2 mo. Norrie disease patients are blind at birth but show loss of hearing at a median age of 12 y (3, 18). The progressive hearing loss in the *Ndp* KO mice was consistent with the observations in humans and was accompanied by an apparent HC phenotype based on the DPOAE. To ask whether the HC phenotype was a direct effect of the lack of *Ndp* on the sensory epithelial cells of the organ of Corti (refer to diagrams in Fig. 1I), we examined HCs in the mutant ears. Instead of the normal Sox2-positive supporting cells and Myo7a-positive HCs of the WT mouse cochlea (Fig. 1J and SI Appendix, Figs. S1 C and E and S2 B and D),

HCs lacking Myo7a were present in cochlear cryosections of the heterozygous and KO ears (SI Appendix, Fig. S2 C, E, and F), and cochlear whole mounts revealed death of OHCs in the base of the cochlea (Fig. 1K). Computational sections including YZ and XZ views are shown in each genotype and confirmed the occurrence of Myo7a-negative OHCs adjacent to Sox2-positive Deiters' cells. In the apex of the male KO mouse cochlea, IHCs were Myo7a negative (SI Appendix, Fig. S1D).

In the female heterozygous mouse cochlea, OHCs lost Myo7a expression in the nuclear layer, while the protein continued to be expressed in the cuticular plate in the base (SI Appendix, Fig. S1F). The abnormal expression of Myo7a in these OHCs was confirmed in computational sections. In the female KO mouse cochlea, HCs in both the base and apex were negative for Myo7a in the nuclear layer, and death of some OHCs was observed

in the base (*SI Appendix, Fig. S1G*). Computational sections showed Myo7a-negative HCs in both the base and the apex.

The decreased number of OHCs in the KO cochlea was significant in the base (Fig. 1*L*), while there was no significant decrease in surviving IHC numbers (Fig. 1*N*). The number of Myo7a-positive OHCs in the base of the KO cochlea was significantly decreased, while the number of Myo7-positive IHCs was significantly decreased in the apex (Fig. 1*M* and *O*). These losses were reflected in the changes in cochlear function, which were driven by both ABR and DPOAE in basal (higher frequency) regions where abnormal and missing OHCs were focused (40-dB shift in the ABR at 8 kHz with a 20-dB contribution from the DPOAE). The auditory threshold changes in the apical (lower frequency) regions where the changes in IHCs were most pronounced resulted in similar shifts in both metrics (10-dB shift in the ABR at 32 kHz accounted for by a 10-dB shift the DPOAE). From these observations, it appeared that the Myo7a-negative HCs and death of OHCs were responsible for progressive hearing loss in the Norrie disease model.

Expression of Ndp and its Receptor Fzd4 in the Adult Cochlea. To further explore possible abnormalities in the inner ear vasculature, we examined cochlear endothelial cells in the mutant ears. Cd31, a marker for endothelial cells in the vasculature, was observed in the lateral wall and under the organ of Corti (see diagrams in Fig. 1*I* and *SI Appendix, Fig. S2A*). In cryosections at 2 mo, no enlarged or obviously abnormal vessels were observed in the stria vascularis or spiral ligament or in the capillaries directly beneath the organ of Corti in the male *Ndp* KO, female heterozygous, or female KO cochlea (*SI Appendix, Fig. S2 B–F*). This suggests that the HC phenotypes described at 2 mo occur without obvious abnormalities in endothelial cells in the lateral wall.

To further investigate the cellular dynamics of ligand receptor activity in the cochlea and to determine whether the absence of *Ndp* affects the organ of Corti directly, we assessed the location of Ndp and Fzd4, the reported receptor for secreted Ndp (11, 13). At P28, Ndp was expressed in cells of the inner and outer sulcus and in supporting cells, including Deiters', Hensen's, and Claudius' cells, but not HCs (Fig. 2*A* and *B*). Strong *Fzd4* in situ signal was detected in OHCs, Deiters', and inner border cells (Fig. 2*C*). This suggested that Ndp secreted from the inner sulcus and supporting cells could activate Fzd4 on HCs. Ndp expression was also seen in the spiral ligament. *Fzd4* messenger RNA (mRNA) was expressed in endothelial cells in the stria vascularis at P28 (Fig. 2*D*). Endothelial cells in the spiral ligament were positive for *Fzd4* mRNA, suggesting that Ndp secreted from cells of the lateral wall could stimulate Fzd4 on endothelial cells in the spiral ligament.

As no phenotype was observed in endothelial cells in the *Ndp* KO mouse cochlea at 2 mo, we evaluated endothelial cells in the lateral wall at an older age. Endothelial cells in the stria vascularis of KO mice at 6 mo had no obvious morphological abnormalities; however, endothelial cells in the spiral ligament of KO mice at 6 mo were sparse (*SI Appendix, Fig. S3 A and B*).

Expression of Ndp and Fzd4 in the Embryonic and Newborn Cochlea. To further probe the cause of the hearing loss and HC abnormalities in the KO mice, we assessed expression of *Ndp* and its receptor at earlier time points in cochlear development and maturation. At E14, Ndp was expressed throughout the cochlear duct, including the prosensory epithelium (Sox2-positive cells; *SI Appendix, Fig. S4A*). At E18, when the HCs are fully formed, expression of Ndp was observed in the greater epithelial ridge but not in supporting cells or HCs (*SI Appendix, Fig. S4 B and D*). Ndp was also expressed in the outer sulcus but not in the lateral wall at this stage. After birth (P3), Ndp was still expressed strongly in the greater epithelial ridge but not in supporting cells or HCs (*SI Appendix, Fig. S4 C and E*). The stria vascularis,

comprising marginal cells, intermediate cells, and basal cells, expressed Ndp only in basal cells at P3.

We investigated the expression site of *Fzd4* mRNA in the developing cochlea by RNAscope in situ hybridization. At E18, *Fzd4* mRNA was weakly expressed in HCs and supporting cells, including inner border, pillar, Deiters', and Hensen's cells (*SI Appendix, Fig. S5A*). In addition to these cells, *Fzd4* mRNA was expressed in endothelial cells under the organ of Corti. *Fzd4* expression in HCs, supporting cells, and endothelial cells increased after birth (P3; *SI Appendix, Fig. S5B*).

In the lateral wall, *Fzd4* mRNA was expressed in endothelial cells in the stria vascularis at P3 (*SI Appendix, Fig. S5C*). In situ staining was compared to a negative control (*SI Appendix, Fig. S5D*). As Ndp was expressed in the greater epithelial ridge (from E18), supporting cells (from P28), basal cells (from P3), and the spiral ligament (from P28), we hypothesized that Ndp secreted from the greater epithelial ridge activated Fzd4 on HCs, and Ndp produced from basal cells stimulated Fzd4 on endothelial cells of the stria vascularis during development.

Altered Distribution of Myo7a HCs in the Base of the *Ndp* KO Cochlea at P3. In cryosections of the cochlea from heterozygous and KO mice at P3, no obvious phenotype was observed in endothelial cells in the stria vascularis or under the organ of Corti (Fig. 3*A* and *B* and *SI Appendix, Fig. S6A*). In the KO cochlea, instead of the Sox2-positive supporting cells and Myo7a-positive HCs of the WT mouse cochlea (Fig. 3*C*), immunostaining revealed Myo7a-negative OHCs in the base in surface view and in computational sections (Fig. 3*E*). Both supporting cells and HCs were intact in the apex in the WT, heterozygous, and KO ears (Fig. 3*D* and *F* and *SI Appendix, Fig. S6C*). Myo7a-negative OHCs were also found in the basal region of the heterozygous cochlea (*SI Appendix, Fig. S6B*). To rule out a change in the protein that made it unreactive to the rabbit Myo7a antibody, we compared staining with a mouse Myo7a antibody (*SI Appendix, Fig. S7*). The signal from the rabbit Myo7a antibody overlapped with the signal from the mouse Myo7a antibody, confirming the presence of HCs with altered or absent Myo7a expression in the cochlea from heterozygous and KO mice. To assess the function of Myo7a-negative HCs in the cochlea from the KO mouse, we treated sensory epithelia with fixable FM1-43 and stained with Myo7a. FM1-43 enters cells through active HC transduction channels (19). FM1-43 uptake by both Myo7a-negative and -positive OHCs was found in the KO cochlea at similar levels to the normal cochlea (*SI Appendix, Fig. S8 A and B*). The normal FM1-43 uptake, along with normal DPOAE thresholds and a mild ABR threshold elevation at 1 mo in KO mice, suggests that HCs retain their mechanosensitive function during the early postnatal period.

Expression of Prestin and Espin Is Maintained in HCs of *Ndp* KO Mice. We tested whether other representative HC markers such as prestin and espin were affected in the *Ndp* KO mouse cochlea. Female heterozygous, female KO, and male KO mice at P3 had normal prestin expression in OHCs (*SI Appendix, Fig. S9 A–D*). At 2 mo, WT mice presented normal Myo7a and prestin expression in OHCs (*SI Appendix, Fig. S10 A and C*). OHCs in the KO cochlea, which were negative for Myo7a in the nuclear layer, expressed prestin (*SI Appendix, Fig. S10 B and D*). Espin expression was also intact in HCs of WT, female heterozygous, female KO, and male KO mice at P3 (*SI Appendix, Fig. S11 A–D*), and its expression was confirmed by XZ-plane images (*SI Appendix, Fig. S11 E–H*). Espin expression was maintained in HCs of both the base and apex in KO ears throughout the postnatal and adult stages (*SI Appendix, Fig. S12 A–F*).

To assess the stereocilia bundle morphology, the *Ndp* KO cochlear samples were observed by scanning electron microscopy

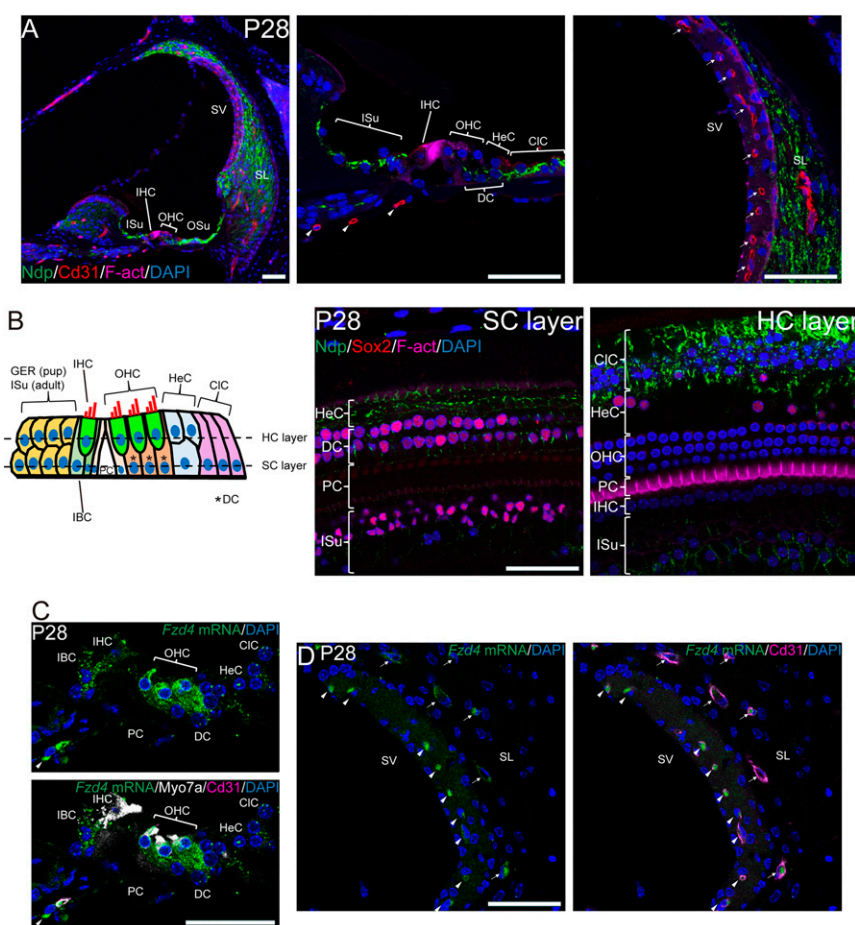


Fig. 2. Expression pattern of *Ndp* and *Fzd4* mRNA in the cochlea at P28. (A) *Ndp* expression was observed widely under the IHCs and OHCs, in the inner sulcus (ISu), outer sulcus (OSu), and spiral ligament (SL) in a cryosection view of the cochlea (Left). High-power view of the organ of Corti (Middle) shows staining of *Ndp* in supporting cells (SCs), including DCs, HeCs, and CICs. *Cd31* (arrowheads) is expressed in endothelial cells lining the capillaries under the organ of Corti. High-power view of the lateral wall (Right) shows *Ndp* expression in the SL and *Cd31*-positive endothelial cells in the vessels of the stria vascularis (SV). (B) Diagram of the organ of Corti with the confocal planes of the SC and HC layers indicated by dashed lines. The SC layer shows *Ndp* expression in the inner sulcus (ISu), DCs, and HeCs, and the HC layer shows *Ndp* expression in the inner sulcus (ISu) and CICs. (C) In situ hybridization showed *Fzd4* mRNA expression in HCs, IBCs, DCs, HeCs, CICs, and endothelial cells under the organ of Corti (arrowhead). *Fzd4* mRNA and DAPI are shown alone (Upper) and merged with *Myo7a* and *Cd31* (Lower). (D) *Fzd4* mRNA was expressed in endothelial cells of the SV and SL. Arrowheads and arrows indicate *Cd31*-positive endothelial cells in the SV and the spiral ligament (SL), respectively. *Fzd4* mRNA and DAPI alone (Left) and merged with *Cd31* (Right). (Scale bars, 50 μ m).

(SEM). No major stereocilia bundle abnormalities in HC bundles were seen in the KO cochlear preparations examined up to 8 wk of age. At these time points, *Myo7a* abnormalities were already long present in a large number of HCs (*SI Appendix*, Fig. S12G).

***Ndp/Fzd4* Signaling Regulates Transcription of *Pou4f3* and *Gfi1* in HCs.**

We next assessed the expression of a selected group of stereociliary bundle genes and genes of HC development. We sorted HCs from the WT, heterozygous, and KO cochlea at P4-6 from *Ndp* KO mice crossed with *Atoh1-GFP* mice and extracted RNA for qRT-PCR. *Myo7a* transcripts were decreased in HCs from the KO cochlea but not the heterozygous cochlea in comparison to the WT cochlea (Fig. 4A). Transcripts of *Slc26a5* (gene for prestin) and *Espn* in HCs were unchanged in the KO (Fig. 4B and C). Mutations in *Myo7a* (*Ush1b*) cause type-I Usher syndrome (20). *Ush1c* and *Ush1g* also contribute to type-I Usher syndrome; recent work showed that *Myo7a*, *Ush1c*, and *Ush1g* form a tripartite complex at upper tip links and that each protein interacts with the others independently (21). Therefore, we also measured mRNA expression levels of *Ush1c* and *Ush1g*, but transcripts of these genes were not affected in HCs from the KO cochlea (Fig. 4D and E).

We tested the expression of genes involved in the signaling cascade of *Ndp/Fzd4* in HCs. We had previously shown that β -catenin up-regulated *Atoh1* expression (22), and *Ndp/Fzd4* signaling stabilizes β -catenin (11), but *Atoh1* mRNA in the *Ndp* KO cochlea was not changed (Fig. 4F). As the HCs degenerated gradually after birth, we assessed the expression of *Pou4f3* and *Gfi1*, genes involved in HC maturation and maintenance (23). Transcripts of *Pou4f3* and *Gfi1* were significantly down-regulated in HCs from the KO cochlea as compared to HCs from the WT

and heterozygous cochlea (Fig. 4G and H). We concluded that an *Ndp/Fzd4/Myo7a*, *Pou4f3*, and *Gfi1* signaling cascade was critical for the full maturation and function of HCs beyond early postnatal age.

***Pou4f3* in *Ndp* KO Mice.** We then assessed how the *Pou4f3* protein expression pattern changed in the *Ndp* KO cochlea during maturation. At P3, all OHCs and IHCs were positive for *Pou4f3* in both the base and apex of the WT cochlea (Fig. 5A and *SI Appendix*, Fig. S13A); however, while all HCs were positive for *Pou4f3* in the apex of the *Ndp* KO cochlea, *Pou4f3*-negative OHCs and IHCs were observed in the base (Fig. 5B and *SI Appendix*, Fig. S13B). At 2 mo, all OHCs and IHCs remained positive for *Pou4f3* in the WT cochlea (Fig. 5C and D and *SI Appendix*, Fig. S13C and D), whereas all HCs lost *Pou4f3* expression in the KO cochlea (Fig. 5E and F and *SI Appendix*, Fig. S13E and F). We conclude that by 2 mo, the HCs lose *Pou4f3* and *Myo7a* expression without loss of prestin or *espin* (see diagrams in Fig. 5G).

***Ndp* Regulates the Wnt Pathway, Nuclear Hormone Receptor *Nr4a3*, and Histone Methyltransferase *Setd7*.** To further probe which genes were fluctuating in the *Ndp* downstream signaling pathway, we harvested *Atoh1-GFP* (+) cells from the P4-6 *Ndp* WT and KO cochlea, respectively, to analyze genome-wide changes in transcripts by RNA sequencing (RNA-Seq). We focused on a gene set with adjusted $P < 0.05$ (Fig. 6A). Fig. 6B shows each gene in this set in Venn diagrams according to its function. HCs in the *Ndp* KO cochlea are characterized by the down-regulation of three genes that regulate transcription, *Nr4a3*, *Setd7*, and *Pdcd2*. *Nr4a3* is a member of the nuclear hormone receptor (NHR) superfamily that regulates development, growth, metabolism,

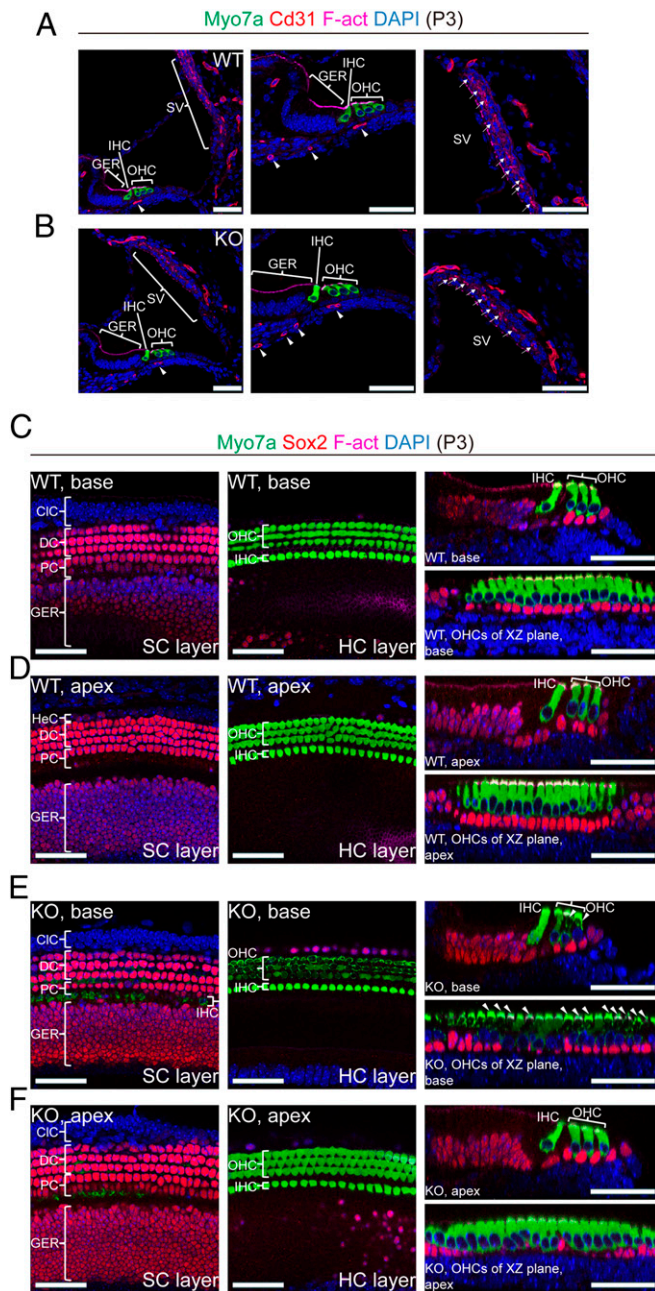


Fig. 3. Myo7a-negative HCs in the *Ndp* KO cochlea. (A and B) Cx31 immunostaining (red) indicates the locations of capillaries in the organ of Corti (arrowheads) and lateral wall in cryosections (Left) from the WT (A) and KO (B) cochlea at P3. Arrowheads indicate endothelial cells in a high-power view (Middle) of the organ of Corti. Arrows indicate endothelial cells in a high-power view (Right) of the stria vascularis (SV). There were no obvious changes in endothelial cell morphology. (C and D) A WT cochlear sensory epithelium had Sox2-positive (red) supporting cells (Left, SC layer) and Myo7a-positive (green) HCs (Middle, HC layer) in surface views and computational sections (Right) at the base (C) and apex (D) of the cochlea. (E and F) An *Ndp* KO cochlear sensory epithelium had normal supporting cells (Left, SC layer), but both surface views (Middle) and computational sections (Right) showed Myo7a-negative HCs (arrowheads) at the base of the cochlea. (Scale bars, 50 μ m.)

and maintenance (24). This superfamily is expressed in the cochlea. Expression of *Nr4a3* and *Nr4a1* (also a member of the NHR superfamily) was increased after noise exposure (25). *Nr2f2* transcription is regulated by *Pou4f3* in HCs (26). Nr4a3

binds hormone response elements at AAAGGTCA sequences located near promoter regions to facilitate gene expression (24). Nr4a1 binds the same sequence and regulates *Myo7a* transcription based on the chromatin immunoprecipitation (ChIP)–Atlas (27), suggesting that down-regulated *Nr4a3* could cause Myo7a deficiency in HCs. Setd7 is a monomethyltransferase for histone 3 (H3) lysine 4 residue (H3K4me1) (28). Setd7 binds to promoters and installs the H3K4me1 mark to regulate transcription (29) as well as on nonhistone proteins such as p53, Sox2, and Lin28a (30–32). Previous papers indicate the significance of this epigenetic modification on development, pathogenesis, protection, and regeneration in the cochlea (33–35). *Rrbp1*, of which knockdown causes ER stress, leading to reduction of cell viability (36), was down-regulated by Ndp deficiency. ER stress triggers OHC death and sensorineural hearing loss (37). On the other hand, inhibition of ER stress attenuates HC loss (38). We presumed down-regulation of *Rrbp1* to cause HC loss shown in the *Ndp* KO cochlea. Interestingly, *Wdr93* and *Illrap11*, which are known to cause autism spectrum disorder and intellectual disability, respectively (39, 40), disorders also observed in Norrie disease (14), were found in the gene set.

Ndp is an atypical Wnt that regulates downstream gene expression through β -catenin/Tcf/Lef. We asked whether Ndp signaling altered downstream gene expression in common with Wnt signaling. In the gene set, *Adcyap1r1*, *Sla*, *Cntnap4*, *Entpd3*, and *Map3k8* are regarded as Wnt related (15, 41–44). Besides these genes, *Nr4a3*, *Setd7*, *Edil3*, *Adam19* (cochlear development), and *Vav1* (cytoskeleton) are also Wnt related (45–48).

Gene Ontology (GO) analysis using database for annotation, visualization and integrated discovery (DAVID; <https://david.ncicrf.gov>) detected two terms related to Wnt, Wnt signaling pathway ($P = 0.025$, *SI Appendix*, Fig. S14A), and negative regulation of Wnt signaling pathway ($P = 0.035$, *SI Appendix*, Fig. S14B). Among the gene set of the Wnt signaling pathway, we found that *Tcf7l1* and *Tcf7l2* were down-regulated in *Ndp* KO mice, which implies that Ndp controls Wnt/ β -catenin signaling cascade by up-regulation of Tcfs. Similar examples include VBPI which regulates Wnt/ β -catenin through stabilization of Tcf/Lef (49). On the other hand, *Wif1* was up-regulated in *Ndp* KO mice in the list of negative regulation of Wnt signaling pathway. Wif1 binds to Wnt proteins, leading to inhibition of their activities (50). These observations suggest that Ndp positively affects Wnt signaling while also activating modulators of the pathway. Thus, the biological processes regulated by Ndp, such as regulating transcription, angiogenesis, and cochlea development, are executed in correlation with the Wnt signaling pathway.

GO Enrichment Analysis Identifies Gene Sets Correlated with HC Development and Function.

We performed GO enrichment analysis from the RNA-Seq data using gene set enrichment analysis (<https://www.gsea-msigdb.org/gsea/index.jsp>) (51, 52). GO terms for genes significantly down-regulated by *Ndp* deficiency correlated with HC development and function (*SI Appendix*, Fig. S15A), axonemal dynein complex assembly (*SI Appendix*, Fig. S15B), retinoic acid metabolic process (*SI Appendix*, Fig. S15C), and regulation of activin receptor signaling pathway (*SI Appendix*, Fig. S15D). The axonemal dynein complex is associated with microtubules in eukaryotic cilia and flagella. *Tekt2* which contributes to the enrichment is related to microtubule-based kinocilium in HCs (53). *Dnaaf2* and *Dnah5* are HC-specific proteins in the inner ear (54). Moreover, retinoic acid signaling controls the height and number of stereocilia in HC bundles (55).

We also focused on the activin receptor signaling pathway, which is linked to the Wnt pathway. Indeed, among the genes in the list that contribute to the enrichment, *Dact2*, *Smad7*, *Cer1*, *Fstl3*, *Fgf9*, and *Fst* are Wnt-related genes (56–61), and *Acrv2b*, *Fgf9*, and *Fst* function during cochlear development (62–64)

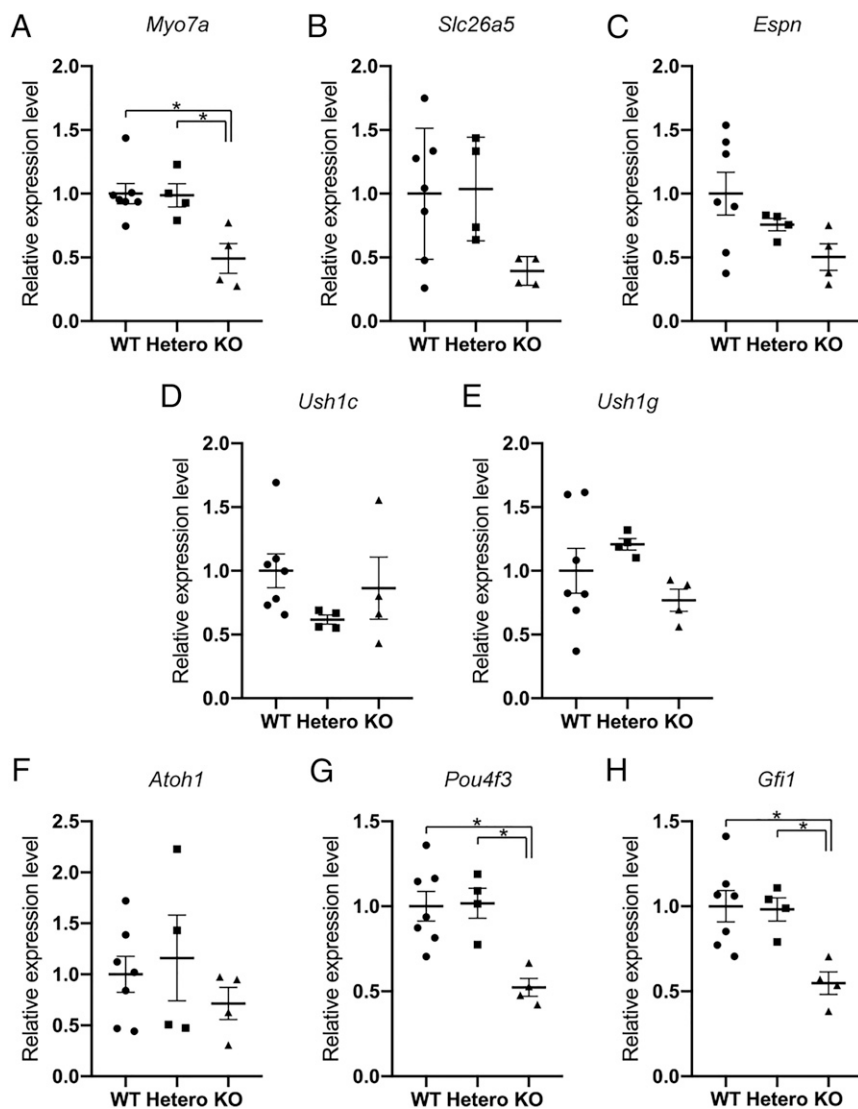


Fig. 4. Altered expression of HC markers in the *Ndp* KO cochlea. (A–H) Expression of genes critical for HC development and function assessed by qRT-PCR in sorted HCs from the *Atoh1-GFP;Ndp* KO mouse cochlea. ANOVA followed by post hoc Bonferroni test revealed that expression levels of *Myo7a*, *Pou4f3*, and *Gfi1* were significantly decreased in HCs from the KO cochlea as compared to the WT and heterozygous cochlea ($P = 0.0052$ for *Myo7a*, $P = 0.0037$ for *Pou4f3*, and $P = 0.0076$ for *Gfi1*). Error bars represent SEs. * $P < 0.01$.

(*Fgf9* and *Fst* are overlapping). The translational initiation gene set suggests an effect of *Ndp* downstream genes in the regulation of protein translation (SI Appendix, Fig. S15E).

Forced Expression of *Ndp* in Sox2-Positive Supporting Cells in *Ndp* KO Mice Rescues *Myo7a* Expression, HC Survival, and Cochlear Function.

The significant degeneration of HCs starting in the early postnatal cochlea and the lack of apparent phenotype in endothelial cells lining the vasculature at that time suggested that the cochlear *Ndp* KO phenotype could be direct rather than secondary to vascular deficiency. In addition, our immunostaining and in situ hybridization studies suggested a ligand–receptor interaction between *Ndp* from supporting cells and the greater epithelial ridge/inner sulcus and *Fzd4* in HCs. We set out to test both hypotheses by a protein replacement strategy.

To accomplish these objectives, we crossed *Z/Norrin* mice, where a floxed *Ndp* cassette is inserted to the *Ubiquitin-b* locus (11) with *Sox2-CreER;tdTomato (Tm)* mice and *Ndp* KO mice to force Sox2-positive supporting cells and the greater epithelial ridge/inner sulcus to express both *Ndp* and *Tm* in *Ndp* KO mice. Because supporting cells and the greater epithelial ridge/inner sulcus are the main site of *Ndp* expression in the organ of Corti (Fig. 2 and SI Appendix, Fig. S4), we overexpressed *Ndp* in

supporting cells and the greater epithelial ridge/inner sulcus, which are the only Sox2-expressing cells in the organ of Corti. We confirmed *Tm* expression in the Sox2-positive cells in *Ndp* KO (X^+Y);*Sox2-CreER;Tm* mice (SI Appendix, Fig. S16A) and both *Tm* and *Ndp* expression in the Sox2-positive cells in *Ndp* KO (X^+Y);*Sox2-CreER;Z/Norrin;Tm* mice (SI Appendix, Fig. S16B) following injection of tamoxifen at P3 and P4. The KO mice showed no *Ndp* expression in the cochlear duct. Sox2-inducible *Tm* expression was observed in supporting cells (pillar cells, Deiters’ cells, Hensen’s cells, and Claudius’ cells), the inner sulcus, and the outer sulcus. Sox2-induced *Ndp* expression was also detected in these *Tm*-positive cells but not in the lateral wall.

We therefore initiated *Tm* expression in *Ndp* KO (X^+Y);*Sox2-CreER;Tm* and both *Tm* and *Ndp* expression in *Ndp* KO (X^+Y);*Sox2-CreER;Z/Norrin;Tm* mice to assess the effect of *Ndp* secretion from cochlear supporting cells and the greater epithelial ridge/inner sulcus in the *Ndp* KO phenotype (see diagram showing this concept in Fig. 7A). Assessment at 2 mo of *Ndp* KO (X^+Y);*Sox2-CreER;Z/Norrin;Tm* showed a statistically significant difference in threshold of the ABR and DPOAE between the KO and overexpression mice at 2 mo (Fig. 7B and C). The *Ndp* KO (X^+Y);*Sox2-CreER;Tm* mice showed a more-severe threshold shift at low frequencies than the male *Ndp* KO mice (Fig. 1B, male 2 mo ABR). We assumed that crossing with other strains

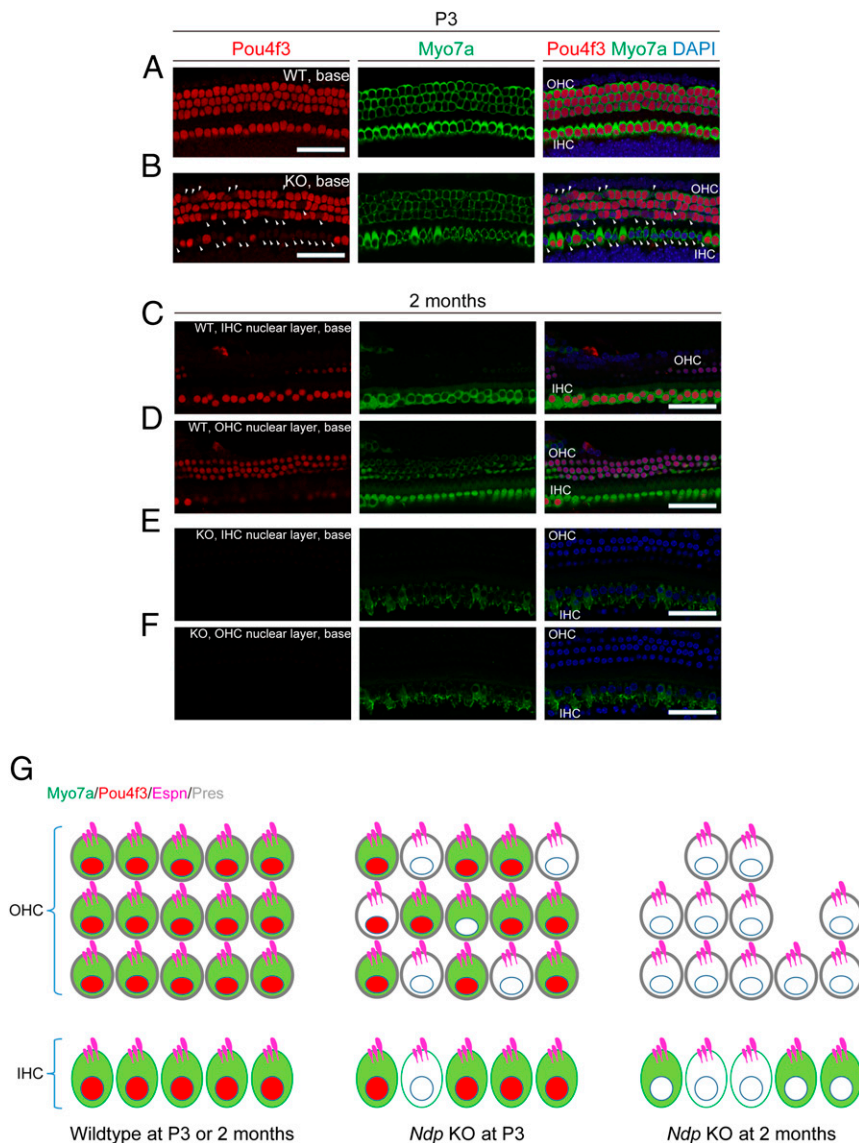


Fig. 5. Pou4f3 expression is lost in HCs in *Ndp* KO cochlea. (A and B) Pou4f3 expression was assessed by immunohistochemistry in the WT and KO cochlea at P3. HCs were positive for Pou4f3 in the base of the WT cochlea (A). Pou4f3-negative HCs (arrowheads) were observed in the base of the KO cochlea (B). (C–F) Pou4f3 expression pattern was evaluated in the WT and KO cochlea at 2 mo. Both IHC and OHC nuclear layers of the base are shown. All IHCs and OHCs in the base of the WT cochlea were positive for Pou4f3 (C and D). Most of IHCs and OHCs in the base of the KO cochlea showed weak or no expression of Pou4f3 (E and F). (Scale bars in A–F, 50 μ m.) (G) Diagram shows the progressive loss of Myo7a from the cytoplasm and Pou4f3 from the nucleus during HC maturation in the *Ndp* KO mouse cochlea. By 2 mo, the KO mouse shows significant OHC loss. Expression of espin (Espn) in the stereociliary bundles and prestin (Pres) in the OHC membrane is maintained.

caused a more-severe threshold shift and measured ABR on *Sox2-CreER;Tm*, *Sox2-CreER;Z/Norrin;Tm*, *Z/Norrin;Tm*, and *Tm* male littermates at 2 mo (SI Appendix, Fig. S17A). The *Sox2-CreER;Tm* and *Sox2-CreER;Z/Norrin;Tm* mice exhibited threshold shifts at low frequencies; while the others showed normal threshold at low frequencies; we thus attributed the more-severe hearing loss to the *Sox2-CreER* transgene. We did not obtain female KO mice from the quadruple cross but did obtain female heterozygous pups, and we measured ABR and DPOAE for *Ndp* (X^+X^-);*Tm*, *Ndp* (X^+X^-);*Z/Norrin;Tm*, *Ndp* (X^+X^-);*Sox2-CreER;Tm*, and *Ndp* (X^+X^-);*Sox2-CreER;Z/Norrin;Tm* ears at 2 mo. There was no significant difference in threshold of ABR and DPOAE between these two models (SI Appendix, Fig. S17B).

In the *Ndp* KO (X^-Y);*Sox2-CreER;Tm* mice, OHCs and some IHCs were negative for Myo7a with OHC death, while few OHCs were positive for Myo7a in the base (Fig. 7D). In the apex of the cochlea, many IHCs were negative for Myo7a (Fig. 7E). These phenotypes were confirmed in computational sections (Fig. 7D and E). In the *Ndp* KO (X^-Y);*Sox2-CreER;Z/Norrin;Tm* ears, the number of surviving OHCs and the number of Myo7a-positive OHCs were significantly increased in the base (Fig. 7F, H, and I). In both the apex and base of the cochlea, the numbers of Myo7a-positive IHCs were significantly increased (Fig. 7G, J,

and K). In summary, forced expression of *Ndp* in *Sox2*-positive supporting cells and the greater epithelial ridge/inner sulcus in *Ndp* KO mice after birth promoted HC survival and retained Myo7a expression in HCs, leading to threshold recovery in the ABR and DPOAE. Despite the increased threshold shift in the *Sox2-CreER* crosses, the thresholds were returned to normal after rescue.

Stabilization of β -catenin in HCs Rescues Cochlear Function in *Ndp* KO Mice.

As already shown in the RNA-Seq data, *Ndp*/Fzd4/ β -catenin signaling pathway is likely concerned with HC maintenance and maturation, we undertook a further set of experiments to test the idea that Wnt signaling in HCs was the cause of the hearing loss. To verify this, we used β -catenin^{lox(Exon3)/+} mice. Exon 3 of β -catenin encodes phosphorylation sites that target GSK3 for degradation. Deletion of exon 3 is induced by *Cre*, and we chose to activate the transgene using *Atoh1-Cre*, which targets the deletion to HCs in the cochlea. By crossing the *Exon3* mice with *Atoh1-Cre* mice, phosphorylation by GSK3 is inhibited in HCs, leading to stabilization of β -catenin. As *Atoh1-Cre* is not inducible, the stabilization of β -catenin begins when *Atoh1* expression is initiated in HCs at E12.5 (65), which is at a different point from

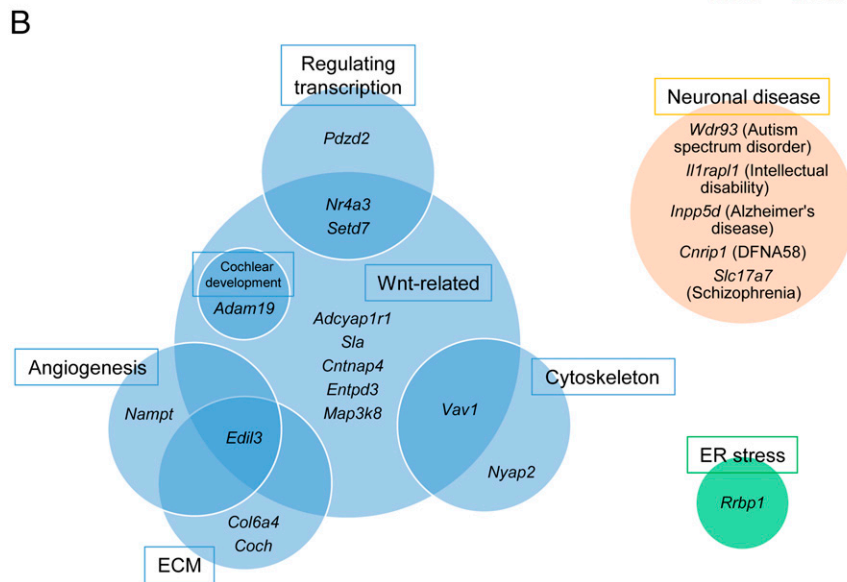
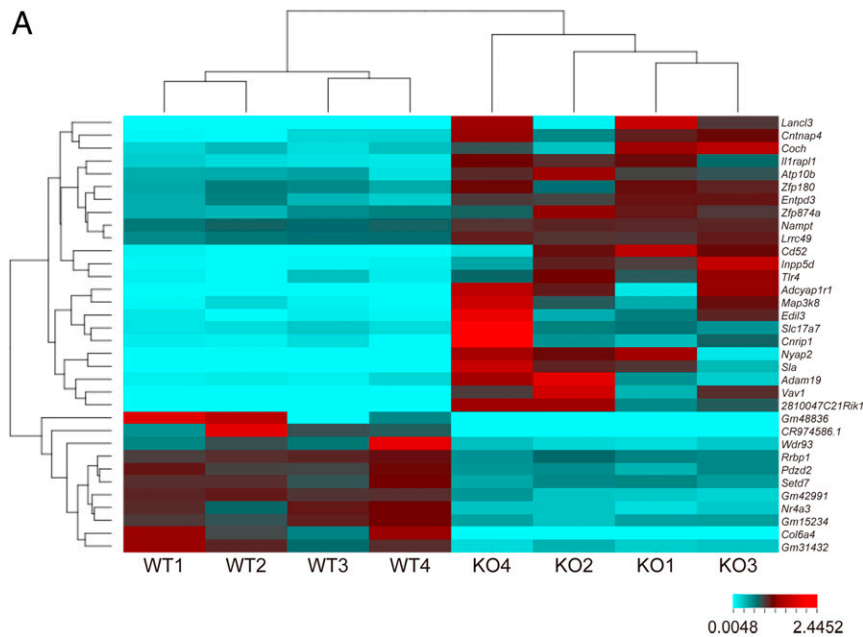


Fig. 6. Differential expression analysis of *Atoh1*-GFP-positive cells in the *Ndp* WT and KO cochleae. (A) Differentially expressed genes from RNA-Seq (adjusted $P < 0.05$) show segregation between WT and *Ndp* KO. (B) Genes with adjusted $P < 0.05$ were analyzed in the Venn diagrams. Groups with significant changes include those regulating transcription (*Pdzd2*, *Nr4a3*, and *Setd7*), angiogenesis (*Namp1* and *Edil3*), ECM (*Col6a4*, *Coch*, and *Edil3*), cytoskeleton (*Nyap2* and *Vav1*), cochlear development (*Adam19*), neuronal disease (*Wdr93*, *Il1rap1*, *Inpp5d*, *Cnrip1*, and *Slc17a7*), and ER stress (*Rrbp1*). Of these, *Nr4a3*, *Setd7*, *Edil3*, *Vav1*, and *Adam19*, shown in the Center of the diagram, were Wnt related, and in addition, other significantly changed genes, *Adcyap1r1*, *Sla*, *Cntnap4*, *Entpd3*, and *Map3k8* were correlated with Wnt signaling.

the *Z/Norrin* strain, where we initiated *Ndp* expression at P3 and P4 by injection of tamoxifen. We then evaluated the *Ndp* KO (X^{-Y});*Atoh1-Cre*;*Exon3* mice physiologically and histologically.

The *Ndp* KO (X^{-Y});*Atoh1-Cre*;*Exon3* mice exhibited significantly lower ABR and DPOAE thresholds at 2 mo of age as compared to the *Ndp* KO (X^{-Y});*Exon3* mice (Fig. 8 A and B), indicating that onset or progression of sensorineural hearing loss could be inhibited by the stabilization of β -catenin in Norrie disease. The *Ndp* KO (X^{-Y});*Atoh1-Cre*;*Exon3* mice also had significantly higher numbers of surviving and *Myo7a*-positive OHCs than the *Ndp* KO (X^{-Y});*Exon3* mice (Fig. 8 C–F). These results show that β -catenin, when provided at sufficient levels, stimulates pathways that normalize *Myo7a* expression and HC activity that in the absence of the *Ndp*/*Fzd4* pathway would be diminished, resulting in hearing loss.

Discussion

Norrie disease is caused by mutations in the *NDP* gene. We show here that an *Ndp* KO mouse had functional abnormalities in cochlear HCs. The dysfunctional HCs showed decreased *Wnt*-related

signaling and loss of nuclear *Pou4f3* protein. Many of the abnormal HCs died between birth and the age of 2 mo, and their death and dysfunction correlated to progressive deafness. We further showed that the HC phenotype could be rescued by *Ndp* replacement by overexpression in supporting cells and cells of the greater epithelial ridge/inner sulcus or by stabilization of β -catenin in HCs of the *Ndp* KO mouse. The rescue by *Ndp* secretion from supporting cells and the greater epithelial ridge/inner sulcus, activating β -catenin in HCs by binding to the *Fzd4* receptor, was consistent with the timing and location that we found for *Fzd4* and *Ndp* expression in the developing and neonatal cochlea. Like the requirement of *Ndp* from supporting cells, *Ndp* was secreted by Müller glia during retinal development and bound to *Fzd4* on retinal neurons (66). We conclude that *Ndp* secreted from supporting cells and the greater epithelial ridge/inner sulcus orchestrates a transcription factor network required for the maintenance and survival of HCs and that the functional requirement of *Ndp* in the cochlea can be replaced by increasing the level of β -catenin, the intracellular effector of

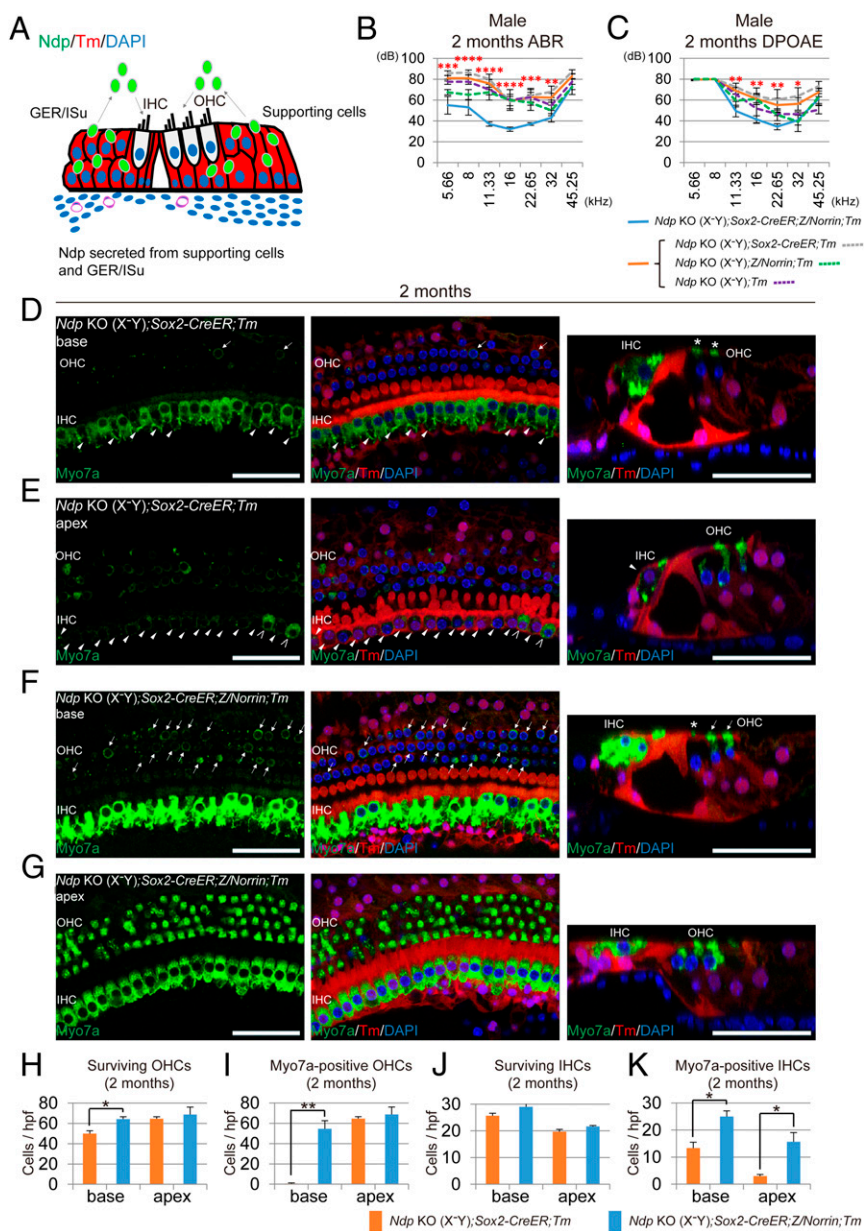


Fig. 7. Forced *Ndp* expression in supporting cells after birth preserves HCs and rescues cochlear function in *Ndp* KO mice. (A) Diagram indicates the secretion of Ndp from Sox2-positive supporting cells and the greater epithelial ridge (GER)/inner sulcus (ISu) in the *Ndp* KO (X^{-Y});*Sox2-CreER*;Z/*Norrrin*;td*Tomato* (*Tm*) ear and the mechanism for Ndp effects on HCs. (B) ABR thresholds showed recovery at 2 mo in *Ndp* KO (X^{-Y});*Sox2-CreER*;Z/*Norrrin*;Tm mice ($n = 5$) as compared to *Ndp* KO (X^{-Y});*Sox2-CreER*;Tm ($n = 7$) and other controls (*Ndp* KO (X^{-Y});Z/*Norrrin*;Tm ($n = 2$) and *Ndp* KO (X^{-Y});Tm ($n = 2$); $P < 0.0001$, ANOVA). Post hoc tests using Fisher's least significant difference (LSD) method revealed significant differences at all frequencies except 45.25 kHz. (C) DPOAE thresholds in *Ndp* KO (X^{-Y});*Sox2-CreER*;Z/*Norrrin*;Tm mice at 2 mo had recovered compared to the *Ndp* KO (X^{-Y});*Sox2-CreER*;Tm and other controls (*Ndp* KO (X^{-Y});Z/*Norrrin*;Tm and *Ndp* KO (X^{-Y});Tm; $P < 0.0001$, ANOVA). Post hoc tests using Fisher's LSD method revealed significant differences at 11.33, 16.00, 22.65, and 32.00 kHz. (B and C) Error bars represent SEs. $*P < 0.05$, $**P < 0.01$, $***P < 0.001$, $****P < 0.0001$ by Fisher's LSD method. (D) Most OHCs and some IHCs (arrowheads) were negative for *Myo7a* in the base of the cochlea of *Ndp* KO (X^{-Y});*Sox2-CreER*;Tm mice (arrows indicate *Myo7a*-positive OHCs). *Myo7a*-negative OHCs are also seen (*) in computational sections (Right). (E) All but a few (Δ) IHCs were negative for *Myo7a* in the apex (arrowheads) as confirmed in computational sections (Right). (F) After forced expression of Ndp in Sox2-positive supporting cells and the greater epithelial ridge (GER)/inner sulcus (ISu) of the *Ndp* KO (X^{-Y});*Sox2-CreER*;Z/*Norrrin*;Tm cochlea, many OHCs survived and retained *Myo7a* expression (arrows). Computational sections (Right) exhibited OHCs negative (*) and positive (arrows) for *Myo7a*. (G) IHCs expressing *Myo7a* were observed in the apex of the cochlea. (Scale bars in D–G, 50 μm.) (H and I) A significant decrease in the number of OHCs (H) and *Myo7a*-positive OHCs (I) at the base of the cochlea in the *Ndp* KO (X^{-Y});*Sox2-CreER*;Tm ($n = 3$) was restored in the *Ndp* KO (X^{-Y});*Sox2-CreER*;Z/*Norrrin*;Tm ($n = 3$) cochlea. (J and K) No loss of IHCs (J) was observed in the *Ndp* KO (X^{-Y});*Sox2-CreER*;Tm cochlea, but a significant decrease in *Myo7a*-positive IHCs (K) in the base and apex of the cochlea in the *Ndp* KO (X^{-Y});*Sox2-CreER*;Tm ($n = 3$) was restored in the *Ndp* KO (X^{-Y});*Sox2-CreER*;Z/*Norrrin*;Tm cochlea ($n = 3$). (H–K) Error bars represent SEs. $*P < 0.05$, $**P < 0.01$ by Student's *t* test.

Wnt signaling. Our data do not rule out the possibility that Ndp secreted from supporting cells indirectly rescued HCs by an effect on vascular function, but the rescue resulting from stabilization of β -catenin in HCs supports a direct effect on HC development.

Myo7a was prominently decreased in the cochlear HCs and resulted in a phenotype similar to that of Usher syndrome type 1B, a deaf-blindness syndrome, and nonsyndromic deafness, DFNB2 and DFNA11 (67–70). *Myo7a* mutant mice, *Myo7a*^{816SB} and *Myo7a*^{GJ} (*shaker-1*), show severely disorganized bundles of HCs, whereas the original *shaker-1* mutant, *Myo7a*^{sh1}, shows normal early development of stereocilia bundles with abnormal cochlear responses, which indicates that *Myo7a* is required for normal stereocilia bundle organization and HC function (71). Our SEM data show HC death but almost no abnormal stereocilia bundles.

Intriguingly, not only *Myo7a* but also other HC markers, such as *Pou4f3* and *Gfi1*, were down-regulated in HCs of the *Ndp* KO cochlea. *Atoh1* is capable of reprogramming supporting cells to

HCs in the early postnatal period (72–76) and is a key gene for HC differentiation and development in the cochlea, acting to up-regulate other genes needed for subsequent steps in differentiation (73, 75, 77–79). Previous work showed that *Pou4f3* was regulated by *Atoh1* (80). *Gfi1* and *Pou4f3* are known components of *Atoh1* downstream signaling and have a role in HC maturation and survival (72, 73, 81, 82). *Myo7a* expression is initiated in IHCs and the first row of OHCs in the base of the cochlea between E14.5 and E15.5, following onset of *Atoh1* expression between E13.5 and E14.5. By E17 and E18, HCs along the entire length of the epithelium express *Myo7a* (83).

Given that most HCs express *Myo7a* at P3 and *Atoh1* is normal at P4–6 in the *Ndp* KO mice, we presume that the abnormal expression of *Pou4f3* and *Gfi1* and the attendant alterations in the distribution (expressed in the cuticular plate but missing in the HC body) of *Myo7a* in the *Ndp* KO mouse cause aberrant HC function, leading to HC death without obvious abnormalities in stereocilia bundles. *Atoh1* expression in HCs is extinguished by P7 (84); maintenance of *Pou4f3* expression could subsequently

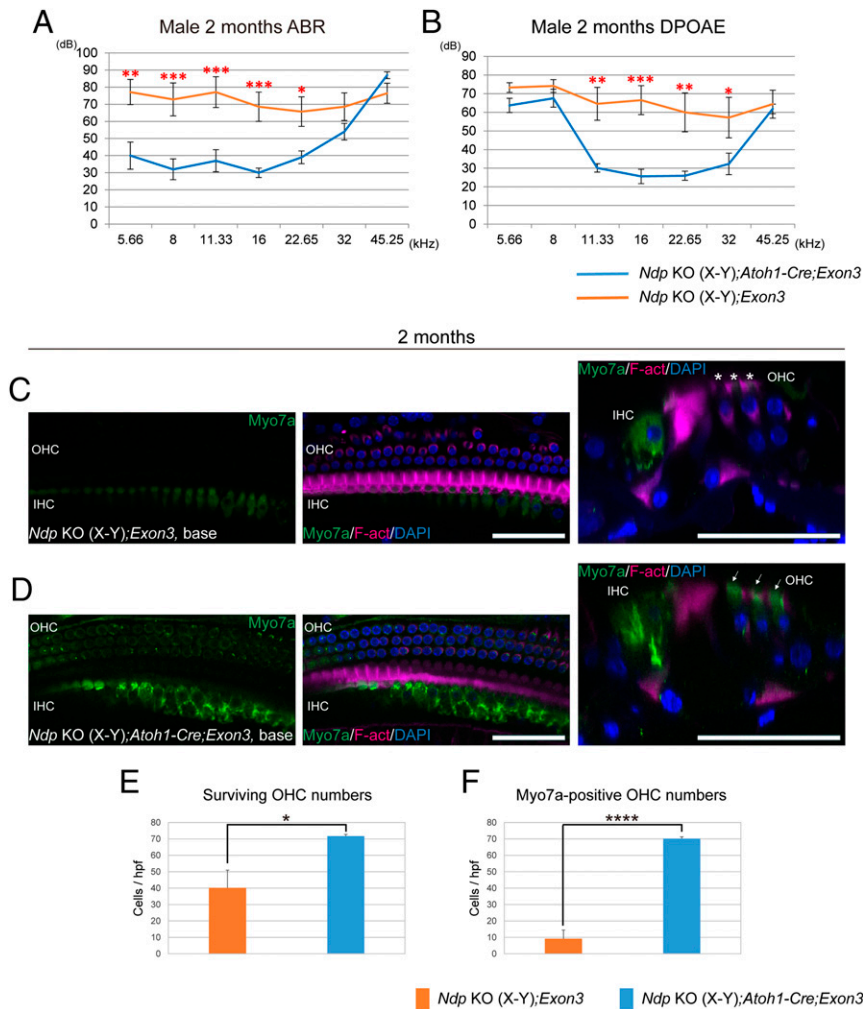


Fig. 8. Stabilization of β -catenin in HCs rescues cochlear function in *Ndp* KO mice. (A and B) *Ndp* KO mice in which β -catenin was overexpressed in HCs by deletion of exon 3 of β -catenin using an *Atoh1-Cre* (*Ndp* KO (X^{-Y});*Atoh1-Cre*; β -catenin^{flox(Exon3)+}; *n* = 5) showed significantly lower ABR (A) and DPOAE (B) thresholds (*P* < 0.0001, ANOVA) than control mice lacking *Atoh1-Cre* (*Ndp* KO (X^{-Y}); β -catenin^{flox(Exon3)+}; *n* = 7). The line with stabilized β -catenin is referred to as *Ndp* KO (X^{-Y});*Atoh1-Cre*;*Exon3* and the control is referred to as *Ndp* KO (X^{-Y});*Exon3*. Post hoc tests using Fisher's least significant difference (LSD) method revealed significant difference at 5.66, 8.00, 11.33, 16.00, and 22.65 kHz in the ABR and 11.33, 16.00, 22.65, and 32.00 kHz in the DPOAE. (C) *Ndp* KO (X^{-Y});*Exon3* mice showed loss of OHCs and loss of Myo7a in surviving OHCs (*) in the base of the cochlea. IHCs were positive for Myo7a. (D) *Ndp* KO (X^{-Y});*Atoh1-Cre*;*Exon3* mice exhibited continued Myo7a immunoreactivity in OHCs (arrows) at the base of the cochlea. (Scale bars in C and D, 50 μ m.) (E and F) The *Ndp* KO (X^{-Y});*Atoh1-Cre*;*Exon3* mice (*n* = 4) showed significantly more surviving (E) and Myo7a-positive (F) OHCs than the *Ndp* KO (X^{-Y});*Exon3* mice (*n* = 5; Student's *t* test). (A, B, E, and F) Error bars represent SEs. **P* < 0.05, ***P* < 0.01, ****P* < 0.001, and *****P* < 0.0001 by Fisher's LSD method or Student's *t* test.

rely upon the transcription factor network downstream of *Ndp*. This could explain the loss of Myo7a and subsequent loss of HCs that begins in the early postnatal stage and continues into adulthood in the *Ndp* KO mice.

Pou4f3, the gene responsible for DFNA15 (85) is a class-IV POU-domain transcription factor (72). *Pou4f3* mutant mice exhibit profound sensorineural deafness, with IHC and OHC loss (86). Our immunohistochemistry experiments showed that the number of Pou4f3-negative HCs increased during the maturation of the *Ndp* KO mice. The *Gfi1* gene encodes a zinc finger transcription factor and cellular protooncogene that promotes proliferation and prevents cell death (87). *Pou4f3*^{-/-} and *Gfi1*^{-/-} mice had immature IHCs and abnormal OHCs (81). *Gfi1* was downstream of *Pou4f3* in OHC but not IHC survival. This could explain why OHCs but not IHCs died in the *Ndp* KO. We therefore concluded that *Pou4f3/Gfi1* signaling was key to the HC maturation and survival pathways affected by the absence of *Ndp*. Gene expression studies on the mutant cochlea showed that the canonical Wnt pathway mediated by β -catenin was central to *Ndp/Fzd4* effects in the cochlea. Indeed, our RNA-Seq data identified an influence of *Ndp* KO on Wnt-related genes and gene sets. Changes in expression of Wnt downstream genes related to Norrie disease included *Nr4a3* and *Setd7* (transcription and epigenetic factors), *Edil3* (angiogenesis), and *Adam19* (cochlear development) and further demonstrate that *Ndp* and Wnt act on a common set of genes. Decreased *Pou4f3* expression is likely to be caused by decreased *Atoh1*, although a binding site for

Tcf7 in the *Pou4f3* locus (ChIP-Atlas; <http://dbarchive.biosciencedbc.jp/kyushu-u/mm10/target/Tcf7.10.html>) indicates a potential effect of β -catenin. Direct control of *Pou4f3* by canonical Wnt signaling is further supported by the rescue of the phenotype by β -catenin stabilization.

Although we did not see an effect on the cochlear vasculature in the early postnatal period, loss of *Ndp* secretion from basal cells in the stria vascularis and later from cells of the spiral ligament disrupted endothelial cell function, as seen by spiral ligament degeneration at the age of 6 mo. Given the previous reports that *Ndp* plays a role in the proliferation, growth, and regrowth of endothelial cells in the retina (88–90), we conclude that *Ndp* has the same role in the cochlear lateral wall. From our morphological examination, it appeared that the vasculature changes in the *Ndp* KO occurred subsequent to the degeneration of HCs, in agreement with previous work, in which *Ndp* or *Fzd4* mutant mice exhibited pathology in the lateral wall at 3 to 4 mo (12, 13). The abnormality in HCs appeared earlier than previously considered: Myo7a-negative HCs appeared in the base of the *Ndp* KO cochlea during early postnatal life. During maturation, Myo7a-negative HCs spread apically, and HCs in the base were lost, coinciding with the loss of Pou4f3 expression in HCs. The onset of HC deterioration was not determined, and differences in time course could be dependent on mouse background strain; in each case, however, severe HC loss was apparent at late time points (12, 13).

Ndp is required for HC development even though Ndp activity is redundant with Wnts. This is not surprising given the known redundancy of Wnt proteins (9, 91–93) and is likely explained by distinct actions of its receptor, Fzd4. Rescue of cochlear function by stabilization of β -catenin in HCs proves that the Ndp/Fzd4 signal can be restored by canonical Wnt signaling. The likely mechanism of Ndp is through β -catenin activation of Tcf/Lef. We showed previously that Tcf/Lef can be activated in postnatal HCs (15). We also showed previously that the differentiation of HCs from supporting cells in the postnatal cochlea (16, 94) and in organoids derived from the cochlear sensory epithelium (95, 96) is driven by Wnt through up-regulation of *Atoh1* (22). The replacement of Ndp activity by Wnt signaling restores the expression of *Myo7a* and the survival of HCs. Ndp signaling is not required for the differentiation of HCs but rather for their full maturation and function. Our experiments shed further light on mechanisms of HC maturation shown previously to require *Gfi1* and *Pou4f3* (73, 82).

These data point the way to a strategy for treatment of Norrie disease. The average age of onset of hearing loss in Norrie

disease is 12 y, consistent with our ABR data that showed threshold elevation in KO mice at 1 mo. Visual loss at birth prompts testing to diagnose the disease, and thus if a therapy for hearing loss in Norrie disease were available, it should be possible to initiate treatment before the onset of hearing loss.

Materials and Methods

Animals, threshold measurement of ABR and DPOAE, immunohistochemistry, RNA in situ hybridization, FM1-43 treatment, SEM, cochlear HC sorting, RNA extraction, qRT-PCR and RNA-Seq, cell counts, and statistical analysis are described in *SI Appendix*.

Data Availability. All study data are included in the article and/or *SI Appendix*.

ACKNOWLEDGMENTS. We thank Ken Hashimoto and Kohsuke Tani for guidance on animals. We thank the Harvard Chan Bioinformatics Core, the Bauer Core Facility of Harvard University, and the Flow Cytometry Core of Massachusetts General Hospital for their expert assistance. This work was supported by the NIH (Grants DC014089 and DC017166) and a Grants-in-Aid for Scientific Research (KAKENHI) Program Grant (15K20240).

- X. Ye, Y. Wang, J. Nathans, The Norrin/Frizzled4 signaling pathway in retinal vascular development and disease. *Trends Mol. Med.* **16**, 417–425 (2010).
- C. Halpin, K. Sims, Twenty years of audiology in a patient with Norrie disease. *Int. J. Pediatr. Otorhinolaryngol.* **72**, 1705–1710 (2008).
- U. F. Luhmann *et al.*, Role of the Norrie disease pseudoglioma gene in sprouting angiogenesis during development of the retinal vasculature. *Invest. Ophthalmol. Vis. Sci.* **46**, 3372–3382 (2005).
- J. Ke *et al.*, Structure and function of Norrin in assembly and activation of a Frizzled 4-Lrp5/6 complex. *Genes Dev.* **27**, 2305–2319 (2013).
- T. Jin, I. George Fantus, J. Sun, Wnt and beyond Wnt: Multiple mechanisms control the transcriptional property of beta-catenin. *Cell. Signal.* **20**, 1697–1704 (2008).
- C. Y. Logan, R. Nusse, The Wnt signaling pathway in development and disease. *Annu. Rev. Cell Dev. Biol.* **20**, 781–810 (2004).
- P. Yin *et al.*, Wnt signaling in human and mouse breast cancer: Focusing on Wnt ligands, receptors and antagonists. *Cancer Sci.* **109**, 3368–3375 (2018).
- B. E. Jacques *et al.*, A dual function for canonical Wnt/ β -catenin signaling in the developing mammalian cochlea. *Development* **139**, 4395–4404 (2012).
- H. Clevers, Wnt/ β -catenin signaling in development and disease. *Cell* **127**, 469–480 (2006).
- P. M. Smallwood, J. Williams, Q. Xu, D. J. Leahy, J. Nathans, Mutational analysis of Norrin-Frizzled4 recognition. *J. Biol. Chem.* **282**, 4057–4068 (2007).
- X. Ye *et al.*, Norrin, frizzled-4, and Lrp5 signaling in endothelial cells controls a genetic program for retinal vascularization. *Cell* **139**, 285–298 (2009).
- H. L. Rehm *et al.*, Vascular defects and sensorineural deafness in a mouse model of Norrie disease. *J. Neurosci.* **22**, 4286–4292 (2002).
- Q. Xu *et al.*, Vascular development in the retina and inner ear: Control by Norrin and Frizzled-4, a high-affinity ligand-receptor pair. *Cell* **116**, 883–895 (2004).
- S. E. Smith, T. E. Mullen, D. Graham, K. B. Sims, H. L. Rehm, Norrie disease: Extraocular clinical manifestations in 56 patients. *Am. J. Med. Genet. A.* **158A**, 1909–1917 (2012).
- A. Samarajeewa *et al.*, Transcriptional response to Wnt activation regulates the regenerative capacity of the mammalian cochlea. *Development* **145**, 10.1242/dev.166579 (2018).
- F. Shi, L. Hu, A. S. Edge, Generation of hair cells in neonatal mice by β -catenin overexpression in Lgr5-positive cochlear progenitors. *Proc. Natl. Acad. Sci. U.S.A.* **110**, 13851–13856 (2013).
- X. Ye, P. Smallwood, J. Nathans, Expression of the Norrie disease gene (Ndp) in developing and adult mouse eye, ear, and brain. *Gene Expr. Patterns* **11**, 151–155 (2011).
- C. Halpin, G. Owen, G. A. Gutiérrez-Espeleta, K. Sims, H. L. Rehm, Audiologic features of Norrie disease. *Ann. Otol. Rhinol. Laryngol.* **114**, 533–538 (2005).
- J. R. Meyers *et al.*, Lighting up the senses: FM1-43 loading of sensory cells through nonselective ion channels. *J. Neurosci.* **23**, 4054–4065 (2003).
- D. Weil *et al.*, Human myosin VIIA responsible for the Usher 1B syndrome: A predicted membrane-associated motor protein expressed in developing sensory epithelia. *Proc. Natl. Acad. Sci. U.S.A.* **93**, 3232–3237 (1996).
- M. Grati, B. Kachar, Myosin VIIa and sans localization at stereocilia upper tip-link density implicates these Usher syndrome proteins in mechanotransduction. *Proc. Natl. Acad. Sci. U.S.A.* **108**, 11476–11481 (2011).
- F. Shi, Y. F. Cheng, X. L. Wang, A. S. Edge, Beta-catenin up-regulates Atoh1 expression in neural progenitor cells by interaction with an Atoh1 3' enhancer. *J. Biol. Chem.* **285**, 392–400 (2010).
- C. Zhong, Y. Fu, W. Pan, J. Yu, J. Wang, Atoh1 and other related key regulators in the development of auditory sensory epithelium in the mammalian inner ear: Function and interplay. *Dev. Biol.* **446**, 133–141 (2019).
- A. M. Olivares, O. A. Moreno-Ramos, N. B. Haider, Role of nuclear receptors in central nervous system development and associated diseases. *J. Exp. Neurosci.* **9**(suppl. 2), 93–121 (2016).
- K. N. Alagramam, R. Stepanyan, S. Jamesdaniel, D. H. Chen, R. R. Davis, Noise exposure immediately activates cochlear mitogen-activated protein kinase signaling. *Noise Health* **16**, 400–409 (2014).
- C. Tornari, E. R. Towers, J. E. Gale, S. J. Dawson, Regulation of the orphan nuclear receptor Nr2f2 by the DFNA15 deafness gene Pou4f3. *PLoS One* **9**, e112247 (2014).
- S. Oki *et al.*, ChIP-Atlas: A data-mining suite powered by full integration of public ChIP-seq data. *EMBO Rep.* **19**, e46255 (2018).
- H. Wang *et al.*, Purification and functional characterization of a histone H3-lysine 4-specific methyltransferase. *Mol. Cell* **8**, 1207–1217 (2001).
- J. Kofent, J. Zhang, F. M. Spagnoli, The histone methyltransferase Setd7 promotes pancreatic progenitor identity. *Development* **143**, 3573–3581 (2016).
- S. Chuikov *et al.*, Regulation of p53 activity through lysine methylation. *Nature* **432**, 353–360 (2004).
- L. Fang *et al.*, A methylation-phosphorylation switch determines Sox2 stability and function in ESC maintenance or differentiation. *Mol. Cell* **55**, 537–551 (2014).
- S. K. Kim *et al.*, SET7/9 methylation of the pluripotency factor LIN28A is a nucleolar localization mechanism that blocks let-7 biogenesis in human ESCs. *Cell Stem Cell* **15**, 735–749 (2014).
- W. S. Layman, J. Zuo, Epigenetic regulation in the inner ear and its potential roles in development, protection, and regeneration. *Front. Cell. Neurosci.* **8**, 446 (2015).
- A. Li *et al.*, Novel compounds protect auditory hair cells against gentamycin-induced apoptosis by maintaining the expression level of H3K4me2. *Drug Deliv.* **25**, 1033–1043 (2018).
- Y. He *et al.*, Inhibition of H3K4me2 demethylation protects auditory hair cells from neomycin-induced apoptosis. *Mol. Neurobiol.* **52**, 196–205 (2015).
- H. Y. Tsai *et al.*, Endoplasmic reticulum ribosome-binding protein 1 (RRBP1) overexpression is frequently found in lung cancer patients and alleviates intracellular stress-induced apoptosis through the enhancement of GRP78. *Oncogene* **32**, 4921–4931 (2013).
- A. Herranen *et al.*, Deficiency of the ER-stress-regulator MANF triggers progressive outer hair cell death and hearing loss. *Cell Death Dis.* **11**, 100 (2020).
- J. Hu *et al.*, ER stress inhibitor attenuates hearing loss and hair cell death in *Cdh23*^{er/er1} mutant mice. *Cell Death Dis.* **7**, e2485 (2016).
- A. M. Alazami *et al.*, Accelerating novel candidate gene discovery in neurogenetic disorders via whole-exome sequencing of prescreened multiplex consanguineous families. *Cell Rep.* **10**, 148–161 (2015).
- H. Jin, R. J. Gardner, R. Viswesvariah, F. Muntoni, R. G. Roberts, Two novel members of the interleukin-1 receptor gene family, one deleted in Xp22.1-Xp21.3 mental retardation. *Eur. J. Hum. Genet.* **8**, 87–94 (2000).
- R. Yu, Z. Cui, M. Li, Y. Yang, J. Zhong, Dimer-dependent intrinsic/basal activity of the class B G protein-coupled receptor PAC1 promotes cellular anti-apoptotic activity through Wnt/ β -catenin pathways that are associated with dimer endocytosis. *PLoS One* **9**, e113913 (2014).
- Y. Wang *et al.*, SRC-like adaptor protein negatively regulates Wnt signaling in intrahepatic cholangiocarcinoma. *Oncol. Lett.* **17**, 2745–2753 (2019).
- C. Li *et al.*, Neurexin superfamily cell membrane receptor contactin-associated protein like-4 (Cntnap4) is involved in neural EGF-like 1 (Nell-1)-responsive osteogenesis. *J. Bone Miner. Res.* **33**, 1813–1825 (2018).
- A. Sebastian *et al.*, Wnt co-receptors Lrp5 and Lrp6 differentially mediate Wnt3a signaling in osteoblasts. *PLoS One* **12**, e0188264 (2017).

45. A. M. Rajalin, P. Aarnisalo, Cross-talk between NR4A orphan nuclear receptors and β -catenin signaling pathway in osteoblasts. *Arch. Biochem. Biophys.* **509**, 44–51 (2011).
46. M. J. Oudhoff *et al.*, SETD7 controls intestinal regeneration and tumorigenesis by regulating Wnt/ β -Catenin and hippo/YAP signaling. *Dev. Cell* **37**, 47–57 (2016).
47. A. Takai *et al.*, Anterior neural development requires Del1, a matrix-associated protein that attenuates canonical Wnt signaling via the Ror2 pathway. *Development* **137**, 3293–3302 (2010).
48. J. Li *et al.*, *Xenopus* ADAM19 regulates Wnt signaling and neural crest specification by stabilizing ADAM13. *Development* **145**, dev158154 (2018).
49. H. Zhang *et al.*, VBP1 modulates Wnt/ β -catenin signaling by mediating the stability of the transcription factors TCF/LEFs. *J. Biol. Chem.* **295**, 16826–16839 (2020).
50. J. C. Hsieh *et al.*, A new secreted protein that binds to Wnt proteins and inhibits their activities. *Nature* **398**, 431–436 (1999).
51. V. K. Mootha *et al.*, PGC-1 α -responsive genes involved in oxidative phosphorylation are coordinately downregulated in human diabetes. *Nat. Genet.* **34**, 267–273 (2003).
52. A. Subramanian *et al.*, Gene set enrichment analysis: A knowledge-based approach for interpreting genome-wide expression profiles. *Proc. Natl. Acad. Sci. U.S.A.* **102**, 15545–15550 (2005).
53. H. Yoon, D. J. Lee, M. H. Kim, J. Bok, Identification of genes concordantly expressed with Atoh1 during inner ear development. *Anat. Cell Biol.* **44**, 69–78 (2011).
54. A. E. Hickox *et al.*, Global analysis of protein expression of inner ear hair cells. *J. Neurosci.* **37**, 1320–1339 (2017).
55. B. R. Thiede *et al.*, Retinoic acid signalling regulates the development of tonotopically patterned hair cells in the chicken cochlea. *Nat. Commun.* **5**, 3840 (2014).
56. S. Wang *et al.*, DACT2 is a functional tumor suppressor through inhibiting Wnt/ β -catenin pathway and associated with poor survival in colon cancer. *Oncogene* **34**, 2575–2585 (2015).
57. S. Edlund *et al.*, Interaction between Smad7 and beta-catenin: Importance for transforming growth factor beta-induced apoptosis. *Mol. Cell. Biol.* **25**, 1475–1488 (2005).
58. M. Katoh, M. Katoh, CER1 is a common target of WNT and NODAL signaling pathways in human embryonic stem cells. *Int. J. Mol. Med.* **17**, 795–799 (2006).
59. S. Kelaini *et al.*, Follistatin-like 3 enhances the function of endothelial cells derived from pluripotent stem cells by facilitating β -catenin nuclear translocation through inhibition of glycogen synthase kinase-3 β activity. *Stem Cells* **36**, 1033–1044 (2018).
60. J. Loke *et al.*, Mutations in MAP3K1 tilt the balance from SOX9/FGF9 to WNT/ β -catenin signaling. *Hum. Mol. Genet.* **23**, 1073–1083 (2014).
61. X. H. Han *et al.*, Regulation of the follistatin gene by RSPO-LGR4 signaling via activation of the WNT/ β -catenin pathway in skeletal myogenesis. *Mol. Cell. Biol.* **34**, 752–764 (2014).
62. J. S. McCullar, S. Ty, S. Campbell, E. C. Oesterle, Activin potentiates proliferation in mature avian auditory sensory epithelium. *J. Neurosci.* **30**, 478–490 (2010).
63. S. H. Huh, M. E. Warchol, D. M. Ornitz, Cochlear progenitor number is controlled through mesenchymal FGF receptor signaling. *eLife* **4**, e05921 (2015).
64. E. J. Son *et al.*, Developmental gene expression profiling along the tonotopic axis of the mouse cochlea. *PLoS One* **7**, e40735 (2012).
65. L. D. Zhao *et al.*, Effects of DAPT and Atoh1 overexpression on hair cell production and hair bundle orientation in cultured Organ of Corti from neonatal rats. *PLoS One* **6**, e23729 (2011).
66. R. Seitz, S. Hackl, T. Seibuchner, E. R. Tamm, A. Ohlmann, Norrin mediates neuroprotective effects on retinal ganglion cells via activation of the Wnt/ β -catenin signaling pathway and the induction of neuroprotective growth factors in Muller cells. *J. Neurosci.* **30**, 5998–6010 (2010).
67. D. Weil *et al.*, Defective myosin VIIA gene responsible for Usher syndrome type 1B. *Nature* **374**, 60–61 (1995).
68. F. Gibson *et al.*, A type VII myosin encoded by the mouse deafness gene shaker-1. *Nature* **374**, 62–64 (1995).
69. T. Hasson, M. B. Heintzelman, J. Santos-Sacchi, D. P. Corey, M. S. Mooseker, Expression in cochlea and retina of myosin VIIa, the gene product defective in Usher syndrome type 1B. *Proc. Natl. Acad. Sci. U.S.A.* **92**, 9815–9819 (1995).
70. T. B. Friedman, J. R. Sellers, K. B. Avraham, Unconventional myosins and the genetics of hearing loss. *Am. J. Med. Genet.* **89**, 147–157 (1999).
71. T. Self *et al.*, Shaker-1 mutations reveal roles for myosin VIIA in both development and function of cochlear hair cells. *Development* **125**, 557–566 (1998).
72. A. Costa, L. M. Powell, S. Lowell, A. P. Jarman, Atoh1 in sensory hair cell development: Constraints and cofactors. *Semin. Cell Dev. Biol.* **65**, 60–68 (2017).
73. A. Costa *et al.*, Generation of sensory hair cells by genetic programming with a combination of transcription factors. *Development* **142**, 1948–1959 (2015).
74. M. C. Kelly, Q. Chang, A. Pan, X. Lin, P. Chen, Atoh1 directs the formation of sensory mosaics and induces cell proliferation in the postnatal mammalian cochlea in vivo. *J. Neurosci.* **32**, 6699–6710 (2012).
75. Z. Liu *et al.*, Age-dependent in vivo conversion of mouse cochlear pillar and Deiters' cells to immature hair cells by Atoh1 ectopic expression. *J. Neurosci.* **32**, 6600–6610 (2012).
76. J. L. Zheng, W. Q. Gao, Overexpression of Math1 induces robust production of extra hair cells in postnatal rat inner ears. *Nat. Neurosci.* **3**, 580–586 (2000).
77. T. Cai *et al.*, Characterization of the transcriptome of nascent hair cells and identification of direct targets of the Atoh1 transcription factor. *J. Neurosci.* **35**, 5870–5883 (2015).
78. T. Cai, M. L. Seymour, H. Zhang, F. A. Pereira, A. K. Groves, Conditional deletion of Atoh1 reveals distinct critical periods for survival and function of hair cells in the organ of Corti. *J. Neurosci.* **33**, 10110–10122 (2013).
79. M. W. Kelley, Regulation of cell fate in the sensory epithelia of the inner ear. *Nat. Rev. Neurosci.* **7**, 837–849 (2006).
80. M. Masuda, K. Pak, E. Chavez, A. F. Ryan, TFE2 and GATA3 enhance induction of POU4F3 and myosin VIIa positive cells in nonsensory cochlear epithelium by ATOH1. *Dev. Biol.* **372**, 68–80 (2012).
81. R. Hertzano *et al.*, Transcription profiling of inner ears from Pou4f3(*ddl/ddl*) identifies Gfi1 as a target of the Pou4f3 deafness gene. *Hum. Mol. Genet.* **13**, 2143–2153 (2004).
82. D. Wallis *et al.*, The zinc finger transcription factor Gfi1, implicated in lymphomagenesis, is required for inner ear hair cell differentiation and survival. *Development* **130**, 221–232 (2003).
83. P. Chen, J. E. Johnson, H. Y. Zoghbi, N. Segil, The role of Math1 in inner ear development: Uncoupling the establishment of the sensory primordium from hair cell fate determination. *Development* **129**, 2495–2505 (2002).
84. K. T. Chonko *et al.*, Atoh1 directs hair cell differentiation and survival in the late embryonic mouse inner ear. *Dev. Biol.* **381**, 401–410 (2013).
85. O. Vahava *et al.*, Mutation in transcription factor POU4F3 associated with inherited progressive hearing loss in humans. *Science* **279**, 1950–1954 (1998).
86. M. Xiang *et al.*, Essential role of POU-domain factor Brn-3c in auditory and vestibular hair cell development. *Proc. Natl. Acad. Sci. U.S.A.* **94**, 9445–9450 (1997).
87. Z. Duan, M. Horwitz, Targets of the transcriptional repressor oncoprotein Gfi-1. *Proc. Natl. Acad. Sci. U.S.A.* **100**, 5932–5937 (2003).
88. J. Zuercher, M. Fritzsche, S. Feil, L. Mohn, W. Berger, Norrin stimulates cell proliferation in the superficial retinal vascular plexus and is pivotal for the recruitment of mural cells. *Hum. Mol. Genet.* **21**, 2619–2630 (2012).
89. A. Ohlmann *et al.*, Ectopic norrin induces growth of ocular capillaries and restores normal retinal angiogenesis in Norrie disease mutant mice. *J. Neurosci.* **25**, 1701–1710 (2005).
90. A. Ohlmann *et al.*, Norrin promotes vascular regrowth after oxygen-induced retinal vessel loss and suppresses retinopathy in mice. *J. Neurosci.* **30**, 183–193 (2010).
91. E. M. Dickins, P. C. Salinas, Wnts in action: From synapse formation to synaptic maintenance. *Front. Cell. Neurosci.* **7**, 162 (2013).
92. J. E. Gleason, E. A. Szyleyko, D. M. Eisenmann, Multiple redundant Wnt signaling components function in two processes during *C. elegans* vulval development. *Dev. Biol.* **298**, 442–457 (2006).
93. C. L. Stoick-Cooper *et al.*, Distinct Wnt signaling pathways have opposing roles in appendage regeneration. *Development* **134**, 479–489 (2007).
94. F. Shi, J. S. Kempfle, A. S. Edge, Wnt-responsive Lgr5-expressing stem cells are hair cell progenitors in the cochlea. *J. Neurosci.* **32**, 9639–9648 (2012).
95. W. J. McLean *et al.*, Clonal expansion of Lgr5-positive cells from mammalian cochlea and high-purity generation of sensory hair cells. *Cell Rep.* **18**, 1917–1929 (2017).
96. D. R. Lenz *et al.*, Applications of Lgr5-positive cochlear progenitors (LCPs) to the study of hair cell differentiation. *Front. Cell Dev. Biol.* **7**, 14 (2019).